Current Biology, Vol. 14, 197–207, February 3, 2004, ©2004 Elsevier Science Ltd. All rights reserved. DOI 10.1016/j.cub.2004.01.030

Initiation of Gastrulation in the Mouse Embryo Is Preceded by an Apparent Shift in the Orientation of the Anterior-Posterior Axis

Aitana Perea-Gomez,[1] Anne Camus,[1] Anne Moreau,[1] Kate Grieve,[3] Gael Moneron,[3] Arnaud Dubois,[3] Christian Cibert,[2] and Jérôme Collignon[1,*]

[1]Laboratoire de Développement des Vertébrés
Institut Jacques Monod
UMR 7592 CNRS
Université Paris 6 et 7
2 place Jussieu
75251 Paris
France

[2]Laboratoire de Morphométrie et Modélisation Moléculaire
Institut Jacques Monod
UMR 7592 CNRS
Université Paris 6 et 7
2 place Jussieu
75251 Paris
France

[3]Laboratoire d'Optique Physique
École Supérieure de Physique et Chimie Industrielles (ESPCI)
CNRS UPR A0005
10 rue Vauquelin
75231 Paris
France

Summary

Background: It is generally assumed that the migration of anterior visceral endoderm (AVE) cells from a distal to a proximal position at embryonic day (E)5.5 breaks the radial symmetry of the mouse embryo, marks anterior, and conditions the formation of the primitive streak on the opposite side at E6.5. Transverse sections of a gastrulating mouse embryo fit within the outline of an ellipse, with the primitive streak positioned at one end of its long axis. How the establishment of anterior-posterior (AP) polarity relates to the morphology of the postimplantation embryo is, however, unclear.

Results: Transverse sections of prestreak E6.0 embryos also reveal an elliptical outline, but the AP axis, defined by molecular markers, tends to be perpendicular to the long axis of the ellipse. Subsequently, the relative orientations of the AP axis and of the long axis change so that when gastrulation begins, they are closer to being parallel, albeit not exactly aligned. As a result, most embryos briefly lose their bilateral symmetry when the primitive streak starts forming in the epiblast.

Conclusions: The change in the orientation of the AP axis is only apparent and results from a dramatic remodeling of the whole epiblast, in which cell migrations take no part. These results reveal a level of regulation and plasticity so far unsuspected in the mouse gastrula.

*Correspondence: collignon@ijm.jussieu.fr

Introduction

Although the formation of the primitive streak at E6.5 is the first overt morphological sign of anterior-posterior (AP) polarity in the mouse embryo [1], it is preceded by dynamic patterning events still poorly characterized at the molecular and cellular levels. One day after implantation, molecular patterning is evident along the proximal-distal (PD) axis of the conceptus [2–4]. Around E5.0, a subset of visceral endoderm cells at the distal tip of the embryo responds to signaling by the TGFβ superfamily member Nodal by expressing a specific repertoire of genes [5]. At the same time, genes later involved in primitive streak formation such as *Nodal* and *Wnt3* are expressed in a ring of proximal epiblast cells abutting the extraembryonic ectoderm [3]. The first symmetry-breaking event in the establishment of AP polarity is the asymmetric movement of distal visceral endoderm cells to a more proximal position close to the extraembryonic boundary. Once this cell population has reached its new position (E5.75), which defines the anterior side of the embryo, it is called anterior visceral endoderm (AVE) [2, 6-8]. Concomitantly, the *Nodal* and *Wnt3* expression domains become restricted to the opposite, i.e., posterior, side of the embryo [3]. This restriction is thought to reflect either a regulation of gene expression in the proximal epiblast or a displacement of proximal epiblast cells toward the posterior side before the onset of gastrulation [2]. Genetic and embryological experiments indicate that AVE cells, which secrete Nodal and Wnt antagonists such as Cer-l, Lefty1, and Dkk1, impart anterior identity on the underlying epiblast by protecting it from the signals that promote the formation of the primitive streak in the posterior epiblast [9–11].

This model, where a proximal-distal polarity is converted into an anterior-posterior polarity, gives a prominent role to the migration of AVE cells in determining the position where the primitive streak will form. Although there is currently little information on the morphology of the embryos at these stages, the model seems to rely on the assumption that at the egg-cylinder stage (E5.0), the mouse embryo is radially symmetrical and the migration of AVE cells toward the anterior pole initiates changes in the embryo's shape leading up to bilateral symmetry. Understanding these events in relation to prestreak embryo morphology will be important to address a number of issues such as why or how AVE cells migrate in a particular direction, whether posterior is specified before AVE migration, and how the primitive streak actually forms.

In contrast to prestreak embryos, the morphology of the midgastrula embryo is well known [1]. It can be described as a flattened cylinder, where the AP axis runs along the medial part of the embryonic region (Figure 1). Transverse sections of midstreak-stage embryos reveal an elliptical outline with two geometrical axes, designated long and short. At this stage, the AP axis, marked by the primitive streak at the posterior pole, is aligned with the long axis.

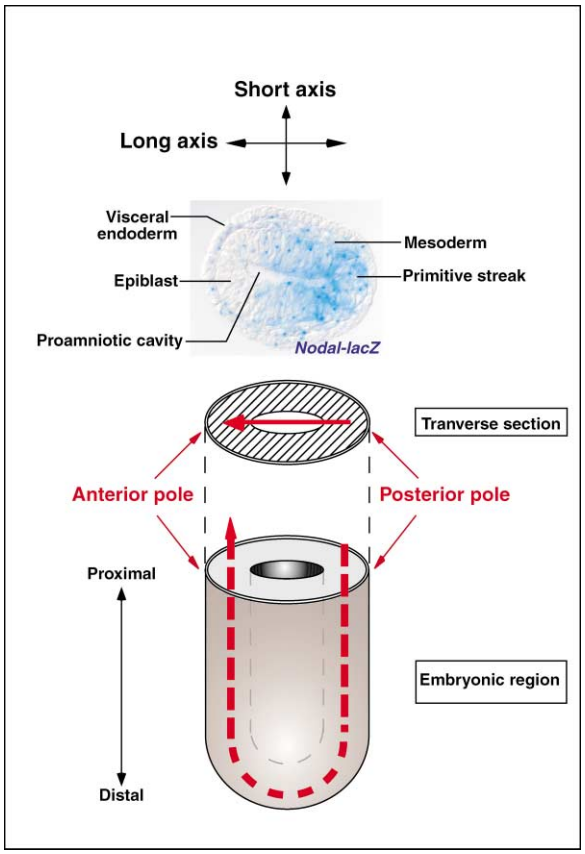

Figure 1. Morphology of the Mouse Embryo at the Midstreak Stage

The mouse embryo has the shape of a flattened cylinder. The AP axis runs along the medial part of the embryonic region. Transverse sections show an ellipsoidal shape with a long and a short axis. Because the AP axis is curved, each transverse section of the embryonic region shows a projection of the AP axis with the primitive streak being positioned at one end of the long axis of the ellipsoid, and the AVE at the other end. For simplicity when describing transverse sections we will write "AP axis" when referring to the projection of the AP axis and "long/short axis" when referring to long/short axis of the ellipsoid shaped transverse section. The picture is a transverse section of a midstreak *Nodal-LacZ* heterozygous embryo showing β-galactosidase activity in the primitive streak and nascent mesoderm cells.

We investigated the molecular patterning of the embryo in relation to its morphology before and around the time of initiation of gastrulation. It is known that the mouse embryo acquires the shape of a flattened cylinder before the formation of the primitive streak [12, 13]. Indeed, transverse sections of prestreak embryos look similar to transverse sections of midstreak embryos except that neither primitive streak nor mesoderm cells have appeared yet. As most of the available information on the events that pattern the pregastrula mouse embryo concerns the behavior and role of AVE cells, we have focused our study on the cellular events taking place in the posterior epiblast.

Here, we report that the orientation of the AP axis of young prestreak embryos is not aligned with the long axis as it is found later during gastrulation but, rather, with the short axis. Within the few hours preceding the onset of gastrulation, the AP axis is shifted toward the long axis in the majority of embryos. Our observations suggest that this shift does not occur to the same extent in all prestreak embryos. As a result, the primitive streak can form in positions unrelated to the geometrical axes of the embryo. We also found that primitive streak formation is associated with a local deformation of the epiblast, resulting in a great variety of embryonic shapes at the initiation of gastrulation. Lineage tracing studies indicate that the change in the orientation of the AP axis with respect to the embryo morphology is due to a change in embryo shape in which cell migrations take no part.

Results

The AP Axis of the Mouse Embryo Is Not Aligned with Its Long Axis at the Prestreak Stage

To establish the relationship between the morphology of the embryo at the prestreak stage and the orientation of the AP axis, whole-mount in situ hybridization was performed on embryos between E6.2–E6.5 using four posterior epiblast markers; the transcription factors Brachyury (T [6, 14]), Goosecoid (Gsc [15, 16]) and Evx1 [17], and the secreted protein Fgf8 [18]; and one AVE marker, the homeoprotein Hex [6, 7]. Histological transverse sections of the stained embryos were analyzed to record the exact position of the expression domains in relation to the morphology of the embryos.

Close inspection of the histological sections confirmed that all the embryos analyzed were at the prestreak stage, as no histological signs of primitive streak formation could be detected. All the embryos showed an ellipsoid shape in transverse sections with a long (123 ± 23.6 μm) and a short axis (77.9 ± 13.1 μm, n = 49) (Figures 2C, 2F, and 2I–2K). The expression domains of posterior and anterior markers could be found at various points between one end of the short axis and one end of the long axis (Figures 2C, 2F, and 2I–2K and data not shown). In some cases, the expression domains of AP markers were located near the ends of the short axis (Figures 2A–2F, n = 18). These results seemed to challenge the assumption that the orientation of the AP axis in prestreak embryos was similar to that of gastrulating embryos, where it is aligned with the long axis.

In order to verify that these observations were not an artifact due to the dissection of the embryos out of the deciduas or their subsequent handling during hybridization procedures, patterns of β-galactosidase activity were analyzed on transverse sections of heterozygous *Nodal-lacZ* embryos kept in utero. The *Nodal-LacZ* allele is expressed in posterior epiblast cells [19, 20]. In agreement with our previous observations, its domain of expression was not always found at the end of the long axis of the prestreak stage embryos analyzed (Figure 2L, n = 9). Similar variations in the position of the expression domains of *Fgf8* and *Hex* with respect to the morphology of prestreak embryos were also obtained in a different mouse line (C57Bl6*CBA F1, n = 8, data not shown).

To assess the relative positions of the anterior and the posterior poles in the same embryo, in situ hybridization

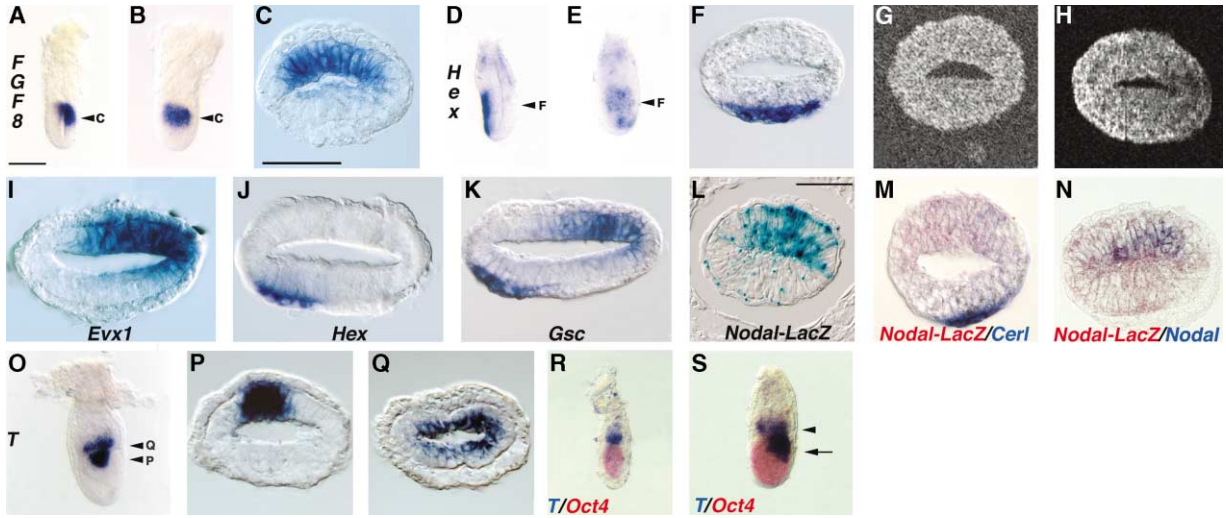

Figure 2. Expression of Anterior-Posterior Markers at the Prestreak Stage

(A–C) *Fgf8* expression in a prestreak stage embryo. (D–F) *Hex* expression in a prestreak stage embryo. (A) and (D) show lateral views of the short axis of the whole embryos. (B) and (E) show lateral views of the long axis of the whole embryos. (C) and (F) are transverse sections of (A and B) and (D and E) respectively, showing *Fgf8* and *Hex* expression at the end of the short axis in the posterior epiblast and in the AVE respectively.

(G and H) Transverse tomographic sections of wild-type (G) and *Nodal* homozygous mutant (H) prestreak embryos obtained by ultrahigh-resolution full-field optical coherence tomography.

(I–K) Transverse sections of prestreak embryos showing expression between the short axis and the long axis of *Evx1* in the posterior epiblast (I), *Hex* in the AVE (J), and *Gsc* in the posterior epiblast and the AVE (K).

(L) Transverse section of a prestreak *Nodal-LacZ* heterozygous embryo in the uterus, stained with X-Gal to reveal β-galactosidase activity.

(M) Transverse section of a prestreak *Nodal-LacZ* heterozygous embryo showing β-galactosidase activity in the posterior epiblast revealed with Salmon-Gal (pink), and *Cer-l* transcripts in the AVE revealed by in situ hybridization (purple). (N) Transverse section of a prestreak *Nodal-LacZ* heterozygous embryo showing β-galactosidase activity in the anterior and posterior epiblast revealed with Salmon-Gal (pink) and *Nodal* endogenous transcripts in the posterior epiblast revealed by in situ hybridization (purple). *Nodal* transcripts are restricted to one end of the short axis.

(O–Q) *T* expression in a prestreak stage embryo. (O) Lateral view of the long axis of the whole embryo. (P) Transverse section showing *T* expression in the posterior epiblast. (Q) Transverse section showing radial *T* expression in the distal extraembryonic ectoderm.

(R) Lateral view of the short axis of a E5.5 embryo showing *T* transcripts (purple) in the extraembryonic ectoderm and *Oct4* transcripts (red) in the epiblast.

(S) Lateral view of the short axis of a E6.5 embryo, showing *T* transcripts (purple) in the extraembryonic ectoderm (arrowhead) and in the posterior epiblast (arrow) and *Oct4* transcripts (red) in the epiblast.

Arrowheads in (A), (B), (D), (E), and (O) show levels of transverse sections. Scale bars are 50 μm. Scale bar in (A) also applies to (B), (D), (E), (O), (R), and (S). Scale bar in (C) also applies to (F)–(K), (M), (P), and (Q). Scale bar in (L) also applies to (N).

was performed on *Nodal-LacZ* heterozygous embryos. The AVE was revealed by the expression of *Cer-l* transcripts [21], and the posterior epiblast was marked by the presence of β-galactosidase activity. In some prestreak stage embryos, we observed the *Cer-l* and *Nodal-LacZ* expression domains at opposite ends of the short axis (Figure 2M, n = 3), indicating that the AP axis of prestreak stage embryos can be perpendicular to the long axis. Similar results were obtained after whole-mount in situ hybridization of wild-type embryos with a probe for *Gsc*, a gene expressed in both the posterior epiblast and the AVE [16, 21]. In all cases examined, the two domains of *Gsc* expression were diametrically facing each other, even when they were between the short and the long axes (Figure 2K, n = 12). Our analyses therefore indicate that although prestreak embryos have bilateral symmetry, the orientation of the AP axis, as defined by the expression of regional markers, is variable with respect to the embryo morphology and is not systematically aligned with the long axis.

In order to determine whether the bilateral symmetry of the prestreak embryo is dependent on the formation of the AP axis, we analyzed the shape of *Nodal* mutant embryos that fail to establish the AP axis [5]. We used a new imaging technique, ultrahigh-resolution full-field optical coherence tomography (URF-OCT), to analyze the shape of intact embryos without histological sectioning [22, 23]. Analysis of transverse tomographic sections confirmed that prestreak stage wild-type embryos show an ellipsoidal shape (Figure 2G, n = 9 out of 9). Interestingly, we found that *Nodal* mutants also show bilateral symmetry at E6.0–E6.5 (Figure 2H; n = 7 out of 9, see Supplemental Data). This finding indicates that prestreak mouse embryos can have an ellipsoidal shape even in the absence of AP polarity, therefore suggesting that the appearance of bilateral symmetry in the postimplantation embryo could precede the emergence of the AP axis.

The Orientation of the AP Axis Changes with Respect to the Morphology of the Embryo before the Onset of Gastrulation

To determine whether the variability in the orientation of the AP axis in the sample population of prestreak

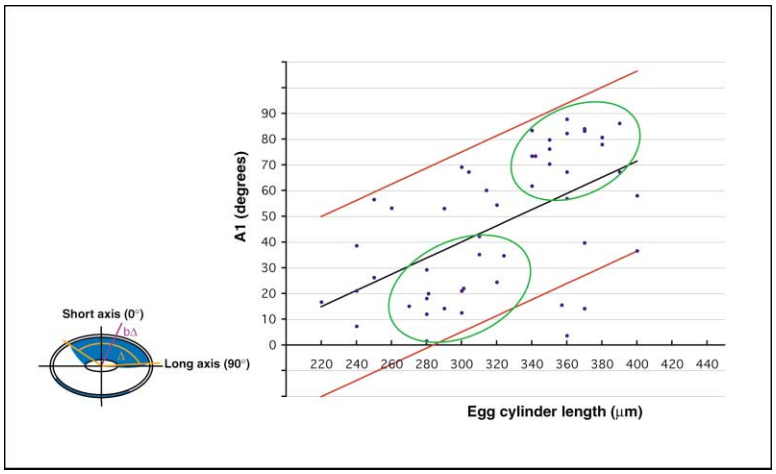

Figure 3. Angular Distribution of AP Axis Orientation in Prestreak Stage Embryos

The value of the angle A_1, represents the angular position of the expression domains of the anterior-posterior markers *Gsc*, *T*, *Evx1*, *Fgf8* and *Hex* in a given embryo. The value of A_1 was calculated as the sum of the homologous Cartesians coordinates of individuals vectors, Vi, defined in each transverse section showing a labeled area. The polar coordinates of each Vi vector are (Δ, bΔ). 0° corresponds to the short axis, 90° corresponds to the long axis. The egg cylinder length was measured from the base of the ecto-placental cone to the distal tip of the embryo. Each blue dot represents an individual embryo. The black line represents the linear regression of the point set. The two red lines define an interval of confidence whose distance to the linear regression equals ±35°. The green ellipses identify a group of young prestreak embryos (egg cylinder length under 330 μm, n = 14) and a group of old prestreak embryos (egg cylinder length over 330 μm, n = 17) defined by a higher density of points in comparison to the rest of the distribution.

embryos could reflect a difference in developmental stages, the angular distribution of the expression domains of posterior and anterior markers was analyzed. For each embryo the position and size of the expression domain was measured on transverse sections and scored as a resulting angle, A_1, comprised between 0° (corresponding to one end of the short axis) and 90° (corresponding to one end of the long axis). In parallel, the length of the egg cylinder was recorded as an indication of developmental time [8, 24, 25]. The results for the different markers were comparable and were therefore treated together.

The angle A_1 was plotted against the length of the egg cylinder (Figure 3). This confirmed that there is a great variability in the angular position of the anterior-posterior markers among prestreak embryos. However, the orientation of the AP axis is not random in relation to embryonic size. In the majority of embryos less than 330 μm in length, presumably at a less-advanced stage than the rest of the sample, the value of A_1 is not more than 60°, indicating that in these embryos the AP axis is never aligned with the long axis (92%, 24 out of 26). In contrast, among embryos more than 330 μm in length, the majority (70%, 16 out of 23) show an A_1 value higher than 60°, indicating that in older prestreak stage embryos the orientation of the AP axis tends to be close to that of the long axis. In order to quantify this observation we calculated the linear regression of the point set. The positive slope of the line indicates that A_1 increases with embryo size, even if the dispersed distribution of the points of the graph results in the correlation coefficient being relatively low (0.56). The majority of the embryos (94%, 46 out of 49) could be included in a band defined arbitrarily by two parallel lines whose distance to the linear regression line equals ±35° (Figure 3). This analysis indicates that the AP axis tends to be away from the long axis in younger prestreak embryos and closer to the long axis in older prestreak embryos.

In younger prestreak embryos the AP axis orientation can be found at any position between 0° (aligned with the short axis) and 70°. However, we could define a subgroup of embryos showing similar characteristics among this wide angular distribution. This group of younger embryos (54%, 14 out of 26) is characterized by an A_1 value found in the inferior half on the interval of confidence defined by linear regression (Figure 3). The mean value of A_1 in this group is 21.7 ± 10.8° and the mean size is 294.6 ± 16.4 μm. Together, these results suggest that in younger prestreak stage embryos the orientation of the emergent AP axis is close to that of the short axis. This finding is in agreement with the observation that the AVE marker *Cer-l* is predominantly expressed at the end of the short axis in prestreak E5.75–E6.0 *Cer-l-GFP* heterozygous embryos (see paper by Mesnard et al., in this issue of *Current Biology*, [40]).

One of the major points of the current model for the establishment of the AP axis in the mouse embryo is that the initial radial expression domains of *Nodal* and *Wnt3* in the proximal epiblast are progressively resolved to the posterior epiblast region where the primitive streak will form [2, 3]. The dynamics of this phenomenon were investigated with respect to the embryo morphology. Because of the stability of the β-galactosidase protein in *Nodal-LacZ* heterozygous embryos, the cells that express *Nodal*, marked both by the presence of *Nodal* transcripts and β-galactosidase protein, can be distinguished from the cells that have ceased to express *Nodal*, which only contain the β-galactosidase protein. Double labeling experiments showed that in a series of prestreak stage *Nodal-LacZ* heterozygous embryos, *Nodal* transcripts and β-galactosidase protein accumulate at one end of the short axis whereas the other end only contains the β-galactosidase protein (Figure 2N, n = 5). This result indicates that the restriction of *Nodal* expression can occur along the short axis of the embryo, further confirming that the emergent AP axis can be aligned with the short axis at the prestreak stage. Moreover, our observation indicates that this restriction involves a fine regulation of *Nodal* expression rather than a directional movement of proximal epiblast cells toward the posterior pole of the embryo.

The first marker reported to be expressed in a ring of proximal epiblast cells abutting the extraembryonic ectoderm and subsequently restricted to the posterior

epiblast was *T* [6, 7]. Interestingly, we have observed that in prestreak stage embryos *T* is expressed in two distinct domains (Figure 2O). Staining is detected in a ring of cells that have the characteristic columnar appearance of extraembryonic ectoderm cells (Figure 2Q) and in a tight domain of posterior epiblast cells (Figure 2P). Double in situ hybridizations at E5.5 and E6.5 show that the ring of proximal cells expressing *T* do not express the epiblast marker *Oct4* [26], confirming they are extraembryonic ectoderm cells (Figures 2R and 2S, n = 4). The extraembryonic ectoderm expression of *T* can be observed until the early-streak stage (Figure 2S). These results demonstrate that *T* is expressed in the extraembryonic ectoderm of E5.5 embryos prior to being activated in a subset of posterior epiblast cells at E6.0.

Taken together, our marker analysis indicates that the emergent AP axis of the prestreak embryo is not aligned with the long axis but tends to be oriented close to the short axis. Subsequently the orientation of the AP axis changes with respect to the morphology of the pregastrula mouse embryo and tends to lie close to the long axis before the onset of gastrulation. Our results suggest that the expression domains of posterior epiblast and AVE markers are shifted concomitantly toward opposite ends of the long axis.

One possible explanation of these observations is that the orientation of the AP axis is shifted toward the long axis as the prestreak embryos grow and approach gastrulation. This shift could be due to a change in gene expression in posterior epiblast and AVE cells or to a movement of these cells toward the long axis. Finally, it could also be explained by a global rearrangement of the morphology of the embryo so that the orientation of the short and long axes change while that of the AP axis remains the same.

The Site of Primitive Streak Formation Is Associated with a Local Deformation of the Epiblast Germ Layer and Cannot Be Predicted by the Morphology of the Prestreak Embryo

Among the oldest prestreak embryos, a subgroup of embryos that shared similar characteristics could be identified (Figure 3). In this group (74%, n = 17 out of 23), A_1 values were found in the superior half of the interval of confidence defined by linear regression. The mean value of A_1 for these embryos was 72.2 ± 18.3°, and the mean size was 360.6 ± 16.6 μm. A minority of old prestreak embryos were not comprised in the group defined above and had A_1 values lower than 60° (26%, n = 6 out of 23). These results indicate that although the AP axis tends to be oriented close to the long axis in older prestreak stage embryos, the orientation of the AP axis with respect to the morphology of the embryo is also variable at this stage. These observations raise the question whether at the time of gastrulation the site of primitive streak formation can always be predicted by the morphology of the prestreak embryo.

It was noticed that some of the prestreak embryos analyzed did not show a characteristic ellipsoidal shape in transverse sections (Figures 4A–4C, 4E, and 4F). These embryos were locally deformed by what appeared as an outgrowth of the epiblast, in which the groove formed by the proamniotic cavity extended. Histological analysis indicates that the epiblast germ layer is not thickened at the site where the deformation appears but, rather, that its shape is locally modified. This deformation was always found in the proximal epiblast region expressing posterior epiblast markers diametrically facing the *Hex* and *Gsc* expression domains in the AVE (Figure 4E and data not shown, n = 11). The mean size of embryos showing a deformation in the epiblast was 370 ± 15.6 μm (n = 11), indicating that these embryos were older than the rest of prestreak embryos. A similar deformation was observed in the primitive streak region of early-streak stage embryos (Figure 4B, 67% n = 4 out of 6, mean size = 418.3 ± 49.3 μm). The deformation of the epiblast was then more pronounced than that of prestreak embryos, and mesoderm cells exiting the primitive streak were found migrating on either side of the apex of the deformation just as they do when the primitive streak is aligned with the long axis. A similar deformation was also observed in transverse sections of early-streak stage embryos inside the uterus (Figures 4C and 4F, 65%, n = 11 out of 17). Taken together, these results suggested that a local deformation of the posterior epiblast at the prestreak stage prefigures the appearance of the primitive streak.

In order to demonstrate that this deformation is not a histological artifact we visualized in three dimensions intact embryos dissected out of the uterus by using URF-OCT. In agreement with the results of the histological analysis, local epiblast deformations were also observed in prestreak and early-streak stage embryos using this technique (Figure 4D, n = 10, see Supplemental Data).

Owing to the diversity in shape of old prestreak embryos (n = 11) and early-streak embryos (n = 23), an accurate measurement of the position of the deformation of the primitive streak could not be obtained. However, two main categories of embryos could be distinguished. The first category comprised embryos where the deformation or the primitive streak were found near the long axis (Figure 4A, 44%, 15 out of 34). The second category was composed of embryos where the deformation or the primitive streak were found at oblique positions (Figures 4B and 4C, 47%, 16 out of 34). In some rare cases the deformation or the primitive streak were found almost at the end of the short axis (Figures 4E and 4F, 9%, 3 out of 34). In these cases, the epiblast deformation resulted in the characteristic shape of an isosceles triangle, with the AVE and the anterior epiblast at the basis of the triangle (Figures 4D–4F). In all other cases the outgrowth of the epiblast at the site of primitive streak formation conferred heterogeneous shapes to the early-streak embryos (Figures 4A–4C).

These findings indicate that the primitive streak tends to form away from the ends of the short axis and are therefore in agreement with the hypothesis that the orientation of the AP axis changes with respect to embryo morphology so that it is shifted away from the short axis and toward the long axis before the onset of gastrulation. Our results also suggest that the site of primitive streak formation cannot be predicted simply from the symmetry of the embryo. What is the relationship be-

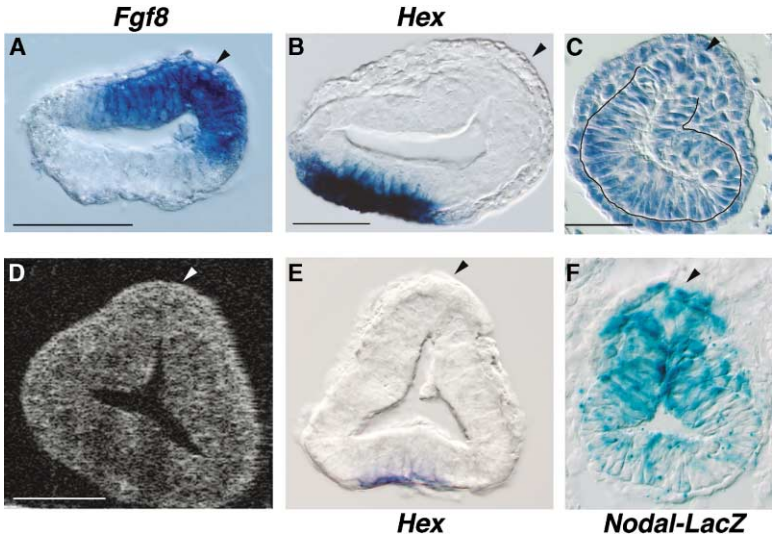

Figure 4. Deformation of the Epiblast Associated to Primitive Streak Formation

(A) *Fgf8* expression on a transverse section of an old prestreak embryo showing a deformation in the posterior epiblast region close to one end of the long axis. (B) *Hex* expression on a transverse section of an early-streak embryo showing a deformation associated to the primitive streak near one end of the long axis. (C) Transverse section of an early-streak embryo inside the uterus showing a deformation associated to primitive streak formation in an oblique position. A black line underlines the contour of the epiblast. (D) Transverse tomographic section of a wild-type old prestreak embryo obtained by ultrahigh-resolution full-field optical coherence tomography. (E) *Hex* expression on transverse section of an old prestreak embryo showing a deformation at the end of the short axis in the posterior epiblast region diametrically facing the AVE. (F) *Nodal-LacZ* expression revealed by X-Gal staining on a transverse section of an early-streak *Nodal-LacZ* heterozygous embryo inside the uterus. The primitive streak is found at the apex of the deformation at one end of the short axis.

Arrowheads indicate the position of the deformation in (A), (D), and (E) and of the primitive streak in (B), (C), and (F). Scale bars are 50 μm. Scale bar in (C) also applies to (F). Scale bar in (D) also applies to (E).

tween the first orientation of the AP axis when it emerges at the young prestreak stage and the site of appearance of the primitive streak at the onset of gastrulation?

Epiblast Cells Located at the End of the Short Axis in Prestreak Embryos Contribute to the Primitive Streak at the Onset of Gastrulation

The position and fate of the posterior epiblast cells located at the end of the short axis at the young prestreak stage was followed in the *Hex-GFP* mouse line [27]. GFP expression in the AVE allowed us to orient *Hex-GFP* heterozygous embryos at the young prestreak stage. In order to identify and label as accurately as possible the posterior epiblast region, we chose to label only embryos in which *Hex-GFP* expression in the AVE was clearly centered at the end of the short axis. We labeled with DiI the posterior epiblast region that was diametrically facing the GFP-positive domain at the end of the short axis. In order to have a reference point, we marked extraembryonic visceral endoderm cells near the embryonic-extraembryonic boundary aligned with the epiblast labeled cells [25] (Figure 5A). The mean size of the embryos at the time of labeling was 283 ± 41 μm, corresponding to the young prestreak stage characterized in the gene expression analysis. Labeled embryos were cultured between 8 and 11 hr to reach the early-streak stage [28] and processed for confocal microscopy. Ten out of 23 labeled prestreak embryos reached the early-streak stage in culture and retained sufficient labeling in the epiblast and extraembryonic VE to be analyzed.

Seven out of ten embryos showed an ellipsoid shape on transverse confocal sections with the primitive streak at one end of the long axis and the AVE cells expressing *Hex-GFP* at the opposite end (Figure 5B″). In the remaining three embryos, the primitive streak was located between the short and the long axis (Figure 5C″). In these cases, the primitive streak was associated with a local deformation of the epiblast, and the AVE cells expressing *Hex-GFP* were found diametrically facing the primitive streak region. This result indicates that the change in the orientation of the AP axis in relation to the morphology of the embryo and the deformation of the epiblast associated with the formation of the primitive streak can be reproduced in in vitro culture in a period of 8 to 11 hr.

In ten out of ten embryos, the relative positions of the DiI-labeled extraembryonic and embryonic cells were not significantly displaced (Figures 5B and 5B″, and 5C and 5C″, Supplemental Data). The posterior epiblast cells located at one end of the short axis at the prestreak stage do not change their position with respect to an extraembryonic landmark suggesting that these cells maintain their absolute position at the time of initiation of gastrulation. Moreover, we found that nine out of ten embryos showed DiI-positive cells in the primitive streak and adjacent nascent mesoderm cells (Figures 5B″ and 5C″). The remaining embryo showed DiI-positive cells in epiblast cells located near the primitive streak region.

In contrast, when we labeled epiblast cells at one end of the long axis of *Hex-GFP* prestreak embryos (showing GFP expression at the end of the short axis), none of the labeled cells contributed to the primitive streak — all were found away from it (data not shown, n = 7 out of 7).

Together, our results indicate that the epiblast cells located at the end of the short axis at the young prestreak stage have a posterior identity and contribute to primitive streak formation close to the ends of the long axis at the early-streak stage. In addition, our results also suggest that posterior epiblast cells keep their absolute position in the embryo from the prestreak to the early-streak stage. Therefore, the change in the orientation of the AP axis with respect to the morphology of the embryo is most likely not due to directional cell movement

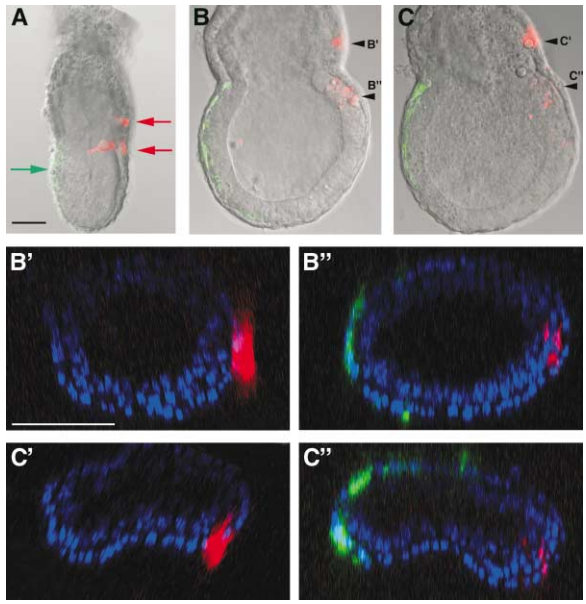

Figure 5. Lineage Tracing of Posterior Epiblast Cells Located at the End of the Short Axis of the Prestreak Stage Embryo

(A) Lateral view of the short axis of a *Hex-GFP* transgenic embryo after DiI labeling. The AVE expressing *Hex-GFP* (green arrow) and the DiI-labeled regions in the posterior epiblast and in the extraembryonic visceral endoderm (red arrows) are at the opposite ends of the short axis.

(B and C) Lateral views of the long axis of *Hex-GFP* transgenic DiI-labeled embryos, after 8 to 11 hr of in vitro culture. Black arrowheads in (B) and (C) indicate the levels of the transverse confocal sections shown in (B′)–(B″) and (C′)–(C″), respectively.

(B′–C″) Transverse confocal sections of embryos shown in (B) and (C). Nuclei are stained with Hoechst. (B′) and (C′) show the extraembryonic VE cells labeled with DiI. (B″) and (C″) show AVE cells expressing *Hex-GFP* and posterior epiblast cells labeled with DiI diametrically facing each other. DiI-labeled posterior epiblast cells have contributed to the primitive streak at the end of the long axis (B″) or in an oblique position (C″).

Scale bar in all panels is 50 μm.

of posterior epiblast cells away from the end of the short axis.

Discussion

New Insights into the Molecular Patterning of the Embryo at the Prestreak Stage

We have found that the restriction of *Nodal* expression from a ring of proximal epiblast cells to the posterior epiblast can occur along the short axis. This observation indicates that the molecular regionalisation of the epiblast that accompanies the emergence of the AP axis can occur along the short axis. In addition, we have found evidence that the restriction of the Nodal expression domain at the prestreak stage reflects regulation of gene expression rather than cell movement. This observation indicates that signals in the prestreak embryo act to maintain Nodal expression in the posterior region and/or to downregulate it in the anterior epiblast. The secreted proteins Cer-l and Lefty1 are Nodal antagonists expressed by AVE cells [21, 29]. These proteins are good candidates to play a role in downregulating *Nodal* expression through local inhibition of the *Nodal* autoregulatory loop in the anterior epiblast [30]. However, the possibility that signals derived from the extraembryonic ectoderm specifically maintain *Nodal* expression in the posterior epiblast cannot be excluded [31].

In the course of our analysis we also found that *T* is expressed in the extraembryonic ectoderm of E5.5 embryos prior to being activated in a subset of posterior epiblast cells at E6.0. This previously unreported expression of *T* in a ring of extraembryonic ectoderm cells persists up to early streak stage at E6.5. Therefore, in contrast to what has been observed in other vertebrate embryos [32], *T* is not exclusively expressed in cells with a mesodermal fate in the mouse embryo. These results suggest that the domain of *T* expression reported in previous studies in the proximal epiblast of E5.5 embryos most likely corresponds to a ring of extraembryonic ectoderm cells [6, 7]. Two types of gene expression patterns in the proximal epiblast can therefore be distinguished. Genes required for primitive streak formation such as *Nodal* and *Wnt3* are first expressed radially and then restricted to the posterior region where they will induce genes involved in mesoderm migration through the streak such as *T* and *Fgf8*. It has been recently shown that signals from the extraembryonic ectoderm are required to pattern the adjacent epiblast [31]. No phenotypes that could be ascribed to a function of *T* in the extraembryonic ectoderm have been reported [14]. Another T box gene, *Eomesodermin*, is also expressed in the extraembryonic ectoderm and in the posterior epiblast. *Eomesodermin* is required before implantation for trophectoderm development, and during gastrulation for cell migration through the primitive streak [33]. It would be of interest to determine the possible genetic interactions between *T* and *Eomesodermin* in the extraembryonic ectoderm at the prestreak stage.

Determination of the Orientation of the AP Axis at the Prestreak Stage

An important question to solve is whether the emergence of the AP axis and, in particular, the migration of AVE cells from distal to anterior positions, causes the appearance of bilateral symmetry (in a previously radially symmetrical embryo). Alternatively, the orientation of the emergent AP axis, close to the short axis, could be influenced by a preexisting bilateral symmetry of the prestreak embryo. Interestingly, we have found that most E6.5 *Nodal* homozygous mutants also show an ellipsoid shape with a long and a short axis in transverse sections. These mutants fail to specify the AVE and do not express posterior epiblast markers such as *Wnt3* or *T* [5]. Thus in *Nodal* mutants the specification of AVE cells and the presence of proximodistal patterning are not required for the existence of morphological bilateral symmetry. This observation suggests that the appearance of bilateral symmetry might precede in time the migration of AVE cells and the emergence of the AP axis. In agreement with this hypothesis, it has been recently shown that the visceral endoderm thickening corresponding to migrating AVE cells is aligned with the short axis of bilateral symmetry in E5.5 embryos [8]. Studies aiming to identify the cues involved in the directional

migration of AVE cells should therefore take into account the morphology of the prestreak embryo.

Such cues could be inherited from early patterning events occurring during preimplantation development. The study of landmarks in the mouse preimplantation embryo has linked the spatial organization of the zygote to that of the early blastocyst (E3.5) [4, 34], but the link between the symmetry of the preimplantation embryo and the orientation of the AP axis in postimplantation embryos remains elusive [35]. A thorough histological analysis has shown that the bilateral symmetry of the early postimplantation embryo (E4.75) relates to the bilateral symmetry of the late implanting blastocyst (E4.5) [13]. However, the relationships between the morphology of the late blastocyst and that of the early blastocyst (and therefore that of the zygote) and between the early postimplantation embryo and the prestreak E6.0 embryo are currently unknown. Lineage tracing studies will be required to draw a clear picture of the correspondence between the short and long axes of preimplantation and postimplantation embryos.

The Orientation of the AP Axis Is Shifted toward the Long Axis before the Onset of Gastrulation

We have shown that the orientation of the AP axis changes with respect to the embryo morphology before the onset of gastrulation. In younger prestreak-stage embryos the AP axis, as assessed by the expression of anterior-posterior markers, tends to be oriented close to the short axis, whereas in the oldest prestreak embryos analyzed the AP axis is oriented close to the long axis. In addition, in early-streak embryos, the primitive streak is found more often in epiblast regions located close to the long axis than to the short axis. Together, these results suggest that the orientation of the AP axis is shifted toward the long axis as the prestreak embryos reach the time of initiation of gastrulation and are in agreement with the findings reported in Mesnard et al. [40]. The amplitude and the directionality of the shift could not be assessed for individual embryos. Given the variability in the position of the AP axis in young prestreak embryos and taking into account the growth of the embryo over this period, we cannot exclude the possibility that the amplitude could vary between embryos and be quite small for some.

Three nonexclusive mechanisms could account for the shift in the orientation of the AP axis in prestreak embryos. This shift could be due to a directional movement of posterior epiblast and AVE cells toward opposite ends of the long axis (Figures 6C-a). Another possibility could be a progressive change in gene expression so that posterior epiblast markers and AVE markers would be down-regulated in cells close to the ends of the short axis, and up-regulated in cells closer to the long axis (Figure 6Cb). Finally, it could result from a global rearrangement of embryo morphology where the positions of the long and short axis would themselves be shifted relatively to an invariant AP axis (Figure 6Cc). As this last mechanism would not involve any change in the position or the gene expression of cells of the posterior epiblast and AVE, the shift in the orientation of the AP axis with respect to the embryo morphology would only be apparent.

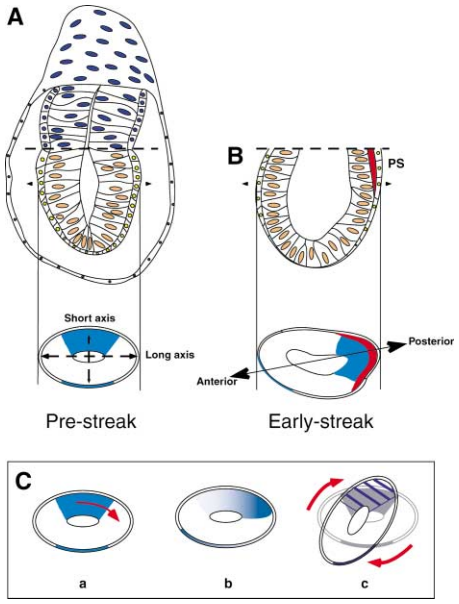

Figure 6. Remodeling of the Mouse Embryo around the Time of Initiation of Gastrulation

(A) In young prestreak-stage embryos, the orientation of the AP axis tends to be aligned with the short axis.

(B) At the early-streak stage, the primitive streak forms more often away from the ends of the short axis. Primitive streak formation in an oblique position is preceded and then associated with a deformation of the posterior epiblast.

(C) The orientation of the AP axis is shifted from the short axis toward the long axis between the young prestreak stage and the old prestreak stage. (a–c) Three possible mechanisms for this shift. (a) Directional movement of posterior epiblast and AVE cells toward opposite ends of the long axis. (b) Change in gene expression patterns in the epiblast and in the VE so that posterior epiblast and AVE markers are downregulated in cells close to the short axis and upregulated in cells closer to the long axis. (c) Global morphological rearrangement. The orientation of the short and long axes is shifted but the cellular composition of anterior and posterior territories remains unchanged.

Our lineage-tracing experiments indicate that cells located at the end of the short axis in young prestreak embryos contribute to primitive streak formation at the early-streak stage and do not significantly modify their absolute positions in the embryo between these two stages. In contrast, cells located at the ends of the long axis at the prestreak stage do not contribute to primitive streak formation at the early-streak stage. These results indicate that the shift in the orientation of the AP axis is most likely due to morphological remodeling rather than directional cell movements of posterior epiblast cells. We cannot exclude the possibility that changes in gene expression may also contribute to the shift in the orientation of the AP axis. To resolve this issue we are currently developing a time-lapse approach to follow gene expression in cultured prestreak embryos.

So far our results support a mechanism whereby the global morphology of the embryo is rearranged, resulting in a reorientation of the short and long axes before gastrulation while the absolute orientation of the AP axis remains unchanged (Figure 6Cc). The driving force for this global rearrangement could be differential

growth between the regions located at the ends of the short and long axis. Another possibility is that the rearrangement is mediated by changes in cell shape. Coordinated changes in the shape of epiblast cells resulting in their transient recruitment at both extremities of the proamniotic cavity could elicit a conveyor belt-like mechanism. This could drive the rotation of the proamniotic cavity and, therefore, of the long axis, toward the AP axis. The conceptus at this stage is firmly anchored to the surrounding decidual tissue by its extraembryonic region, while its flattened embryonic region remains free in the crypt. As a result a conveyor belt mechanism could contribute to a rotation of prestreak embryos with respect to the uterine axes (A.P.-G., A.C., and J.C., unpublished data, [40]).

Variability in the Site of Primitive Streak Formation at the Onset of Gastrulation

What could be the reason for the shift in the orientation of the AP axis from the short toward the long axis of the embryo? This phenomenon increases the distance between the AVE and the posterior epiblast of the flattened cup-shaped embryo. Therefore, one possibility is that the change in embryo morphology is required to distance the posterior epiblast cells from the effect of the antagonists produced by the AVE, Cer-l, Lefty 1, and Dkk1, which inhibit the action of the primitive streak-inducing factors Nodal and Wnt3 [10, 11]. Alternatively the shift in the orientation of the AP axis with respect to the embryo morphology could be simply a consequence of mechanical constraints associated to the growth of the embryo. Indeed, the growth of a cylinder-shaped structure such as the conceptus, with two concentric cell layers, each one with two types of cell morphology (embryonic and extraembryonic), is likely to generate inner tensions. The type of morphological changes we observed could be the most visible effect of a stress-release mechanism for tensions created while the conceptus is growing.

The shift in the orientation of the AP axis may not occur to the same extent in all embryos, so that at the time of gastrulation the orientation of the AP axis is not the same in all embryos. As there is evidence indicating that the initiation of gastrulation is dependent upon cell number in the epiblast (reviewed in [1]), it is conceivable that some embryos reach the time point of initiation of gastrulation when their AP axis is at a distance from the long axis. Alternatively, the differences in the extent of the apparent shift of the AP axis orientation could be dictated by specific cues present in the uterus or in each individual embryo. Our observations suggest that the shift in the orientation of the AP axis can occur during in vitro culture independently of uterine signals after the young prestreak stage. One attractive possibility is that the variability in the position of the AP axis at the onset of gastrulation is a direct consequence of the different cues possibly influencing the spatial patterning of the mouse embryo at preimplantation stages.

Primitive Streak Morphogenesis

The primitive streak can form in regions located away from the ends of the long axis. We have found that in these cases the appearance of the primitive streak is marked by a local deformation in the posterior epiblast. The deformation of the epiblast precedes the appearance of the primitive streak and the formation of the first mesoderm cells. This is reminiscent of primitive streak formation in the chick embryo when the primitive groove, through which mesoderm cells will delaminate, forms within a thickened region of the epiblast [36]. However, in the mouse the deformation is not due to a thickening of the epiblast germ layer but, rather, to a modification of its shape. One possible mechanism is that the shape of epiblast cells is changed in a way similar to that observed during ventral furrow formation in *Drosophila* [37]. The surface of the apical sides, facing the proamniotic cavity, of epiblast cells would be reduced whereas the surface of the basal sides, facing the visceral endoderm, would be enlarged. This would result in a new "pointed end" in the epiblast germ layer without a change in the relative positions or the proliferation rates of posterior epiblast cells.

Early-streak embryos, where the primitive streak forms in an oblique position between the ends of the long and short axes, transiently lose bilateral symmetry as a result of the epiblast deformation accompanying primitive streak formation. As most embryos regain bilateral symmetry once they have passed the midstreak stage, some regulative mechanism must ensure early morphological asymmetries are just transient and are rapidly compensated. Embryos bearing a mutation in the BMP pathway transducing protein Smad1 seem to present a defect in their ability to recover bilateral symmetry after gastrulation [38]. Interestingly, this defect can be attributed to the lack of Smad1 in extraembryonic lineages, most likely in the visceral endoderm. Growth regulation occurring in the epiblast during early gastrulation in wild-type embryos might therefore be dependent on signals from the adjacent visceral endoderm.

Conclusions

In search of new clues to understand the establishment of anterior-posterior polarity in the mouse embryo we have explored the relationship between the morphology of the prestreak embryo and the orientation of the emergent AP axis as assessed by the expression of molecular markers. We have found that in contrast to what is observed during gastrulation, the AP axis of the young prestreak embryo is not aligned with its long axis but tends to be oriented close to the short axis (Figure 6A). In the majority of old prestreak embryos, the AP axis is oriented close to the long axis indicating that the orientation of the AP axis is shifted toward the long axis during the few hours that precede the onset of gastrulation. Cell lineage studies indicate that this shift does not involve cell movements but could be explained by a global morphological change so that the orientations of the short and long axes rotate before gastrulation (Figure 6C). The extent of the shift appears variable between embryos. Therefore, at the initiation of gastrulation the site of primitive streak formation cannot be simply predicted by the geometrical axes of the embryo but, rather, by the position of the expression domains of posterior epiblast markers. We have characterized a

local deformation of the posterior epiblast associated to primitive streak formation in positions away from the extremities of the long axis (Figure 6B). This explains the great variety of embryonic shapes observed at the early-streak stage.

The results reported here provide new bases to examine the mechanisms controlling AP axis determination and set a framework to assess the relation between preimplantation and postimplantation embryonic axes. Having characterized new steps in the development of the prestreak embryo, this work will allow further dissection of the complex cascade of molecular and morphogenetic events that lead to primitive streak formation in the mouse embryo.

Experimental Procedures

Generation of Wild-Type and Transgenic Embryos

Swiss outbred mice, *Nodal-LacZ* heterozygous knockout mice [20] on a Swiss background and *Hex-GFP* heterozygous transgenic mice [27] on a C57Bl6*CBA background, were maintained with an artificial daylight time between 7 a.m. and 7 p.m. Gestation (E0.0) was considered to have begun at midnight before the morning when a copulation plug was found. Prints of pictures taken under a Leica binocular were used to measure the length of the embryos from the base of the ectoplacental cone to the distal tip of the embryonic region. Prints of pictures of transverse sections taken under a Leica microscope were used to measure the length of the short and long axes in the widest region of the embryonic part of the egg cylinder. In situ hybridization, β-galactosidase staining, and histology were performed according to standard methods (see Supplemental Data).

Angular Distribution of Labeled Regions

The angular distribution of the position of the expression domains of posterior and anterior markers of prestreak stage embryos was measured on transverse sections. We defined a system of reference on the ellipsoid-shaped transverse section whose abscissas were parallel to the short axis. For each transverse section showing a labeled area we defined a vector, V_i, whose polar coordinates (R,θ) equal Δ and $b\Delta$, respectively. Δ is the value of the angle of the labeled sector (Δ), calculated as the absolute value of the difference of the angles of its boundaries. $b\Delta$ is the bisector of Δ. We then calculated the Cartesian coordinates of V_i (Xv_i, Yv_i). To determine the angle of orientation of the labeled volume within the whole embryo in the same reference system (A_1), we calculated the sum of the homologous Cartesian coordinates of each V_i. A_1 was given by the following equation:

$$A_1 = \tan^{-1}\left(\frac{\sum_i Y_{Vi}}{\sum_i X_{Vi}}\right)$$

A_1 was comprised between 0° and 360°. No statistical differences in the distribution of A_1 in the four angular sectors (0°–90°, 90°–180°, 180°–270°, and 270°–360°) were observed. Therefore, for simplicity, we calculated the value of A_1 to be comprised between 0° (corresponding to one end of the short axis) and 90° (corresponding to one end of the long axis).

Ultrahigh-Resolution Full-Field Optical Coherence Tomography

This new imaging technique, based on white-light interference microscopy, has been developed at the optics laboratory at ESPCI [22, 23] and is somewhat similar to traditional optical coherence tomography (OCT) [39]. This interferometric technique measures the amplitude of the light backscattered by the sample. In contrast to confocal microscopy, the parameters that govern the transverse and axial resolutions are independent. The transverse resolution is related to the numerical aperture of the objectives. We use microscope objectives with 0.3 NA, providing a transverse resolution of 1.5 μm. The coherence length of the illumination source determines the axial resolution. We measured an axial resolution of 0.9 μm. Prestreak and early-streak stage embryos were fixed in 4% paraformaldehyde/PBS. The embryos were placed lying on one side so as to obtain sagital tomographic images with ~1 μm thickness. Visual C++ software has been developed for image acquisition control, calculation, and display of the tomographic images in real time. Sections in transverse and frontal orientations were then calculated from the three-dimensional data set and movies were made from the series of sections. The images are presented in logarithmic scale, using 256 gray levels.

DiI Labeling and Embryo Culture

Hex-GFP transgenic embryos obtained from matings of *Hex-GFP* transgenic males with C57Bl6*CBA F1 females were dissected in DMEM containing 15% foetal calf serum and 25 mM Hepes. DiI ($DiIC_{18}$[3], Molecular Probes) prepared as a 0.5 mg/ml solution in sunflower oil was injected in epiblast or extraembryonic visceral endoderm regions using an oil pump (Eppendorf). Labeled embryos were cultured in 8-well chamber slides (Nunc) in 75% rat serum/50 μg/ml penicillin,streptomycin/DMEM at 37°C in 5% CO2 in air. At the early-streak stage (after 8–11 hr of culture) labeled embryos were fixed in 4% paraformaldehyde, stained with the nuclear dye Hoechst 33342 (Molecular Probes, 0.05 μg/ml in PBS/0.02%Tween-20), and kept in 25%glycerol/PBS before being observed by confocal microscopy (see Supplemental Data).

Supplemental Data

Supplemental Data including three supplemental movies made from stacks of tomographic sections of wild-type and *Nodal* mutant embryos and a figure showing posterior views of DiI-labeled embryos are available at http://www.current-biology.com/cgi/content/full/14/3/197/DC1/.

Acknowledgments

We are grateful to Drs. T. Rodriguez and S. Srinivas for providing *Hex-GFP* transgenic mice; to Drs. K. Lawson and R. Pederson for enlightening discussions; to Drs. R. Beddington, M. Blum, P. Gruss, R. Harvey, B. Herrmann, I. Mason, and A. Smith for generous gifts of probes; and to Drs. S. Darras and S. Srinivas for advice on DiI-labeling experiments. We would like to acknowledge C. Chamot, A. Troullier, G. Geraud, M. Tramier, T. Piolot, and M. Coppey for help with multiphoton confocal microscopy and S. Paturance for help with rat serum preparation. We also thank D. Mesnard and Dr. M. Zernicka-Goetz for helpful suggestions on the measure of angular distributions and for sharing results prior to publication. This work was supported by grants to J.C. from the Centre National de la Recherche Scientifique (ATIPE), the Ministère de la Recherche (ACI), the Fondation pour la Recherche Médicale, and the Association pour la Recherche contre le Cancer (ARC 5456, 7615). A.P.-G. was supported by a postdoctoral fellowship from the ARC. A.C. was supported by a postdoctoral fellowship from the FRM.

Received: August 22, 2003
Revised: January 1, 2004
Accepted: January 1, 2004
Published: February 3, 2004

References

1. Tam, P.P., and Behringer, R.R. (1997). Mouse gastrulation: the formation of a mammalian body plan. Mech. Dev. *68*, 3–25.
2. Beddington, R.S., and Robertson, E.J. (1999). Axis development and early asymmetry in mammals. Cell *96*, 195–209.
3. Lu, C.C., Brennan, J., and Robertson, E.J. (2001). From fertilization to gastrulation: axis formation in the mouse embryo. Curr. Opin. Genet. Dev. *11*, 384–392.
4. Zernicka-Goetz, M. (2002). Patterning of the embryo: the first spatial decisions in the life of a mouse. Development *129*, 815–829.
5. Brennan, J., Lu, C.C., Norris, D.P., Rodriguez, T.A., Beddington, R.S., and Robertson, E.J. (2001). Nodal signalling in the epiblast patterns the early mouse embryo. Nature *411*, 965–969.

6. Thomas, P., and Beddington, R. (1996). Anterior primitive endoderm may be responsible for patterning the anterior neural plate in the mouse embryo. Curr. Biol. *6*, 1487–1496.
7. Thomas, P.Q., Brown, A., and Beddington, R.S. (1998). Hex: a homeobox gene revealing peri-implantation asymmetry in the mouse embryo and an early transient marker of endothelial cell precursors. Development *125*, 85–94.
8. Rivera-Perez, J.A., Mager, J., and Magnuson, T. (2003). Dynamic morphogenetic events characterize the mouse visceral endoderm. Dev. Biol. *261*, 470–487.
9. Kimura, C., Yoshinaga, K., Tian, E., Suzuki, M., Aizawa, S., and Matsuo, I. (2000). Visceral endoderm mediates forebrain development by suppressing posteriorizing signals. Dev. Biol. *225*, 304–321.
10. Perea-Gomez, A., Rhinn, M., and Ang, S.L. (2001). Role of the anterior visceral endoderm in restricting posterior signals in the mouse embryo. Int. J. Dev. Biol. *45*, 311–320.
11. Perea-Gomez, A., Vella, F.D., Shawlot, W., Oulad-Abdelghani, M., Chazaud, C., Meno, C., Pfister, V., Chen, L., Robertson, E., Hamada, H., et al. (2002). Nodal antagonists in the anterior visceral endoderm prevent the formation of multiple primitive streaks. Dev. Cell *3*, 745–756.
12. Snell, G.D., and Stevens, L.C. (1966). Early embryology. In Biology of the Laboratory mouse, E.L. Green, ed. (New York: McGraw-Hill), pp. 205–245.
13. Smith, L.J. (1985). Embryonic axis orientation in the mouse and its correlation with blastocyst relationships to the uterus. II. Relationships from 4 1/4 to 9 1/2 days. J. Embryol. Exp. Morphol. *89*, 15–35.
14. Wilkinson, D.G., Bhatt, S., and Herrmann, B.G. (1990). Expression pattern of the mouse T gene and its role in mesoderm formation. Nature *343*, 657–659.
15. Blum, M., Gaunt, S.J., Cho, K.W., Steinbeisser, H., Blumberg, B., Bittner, D., and De Robertis, E.M. (1992). Gastrulation in the mouse: the role of the homeobox gene goosecoid. Cell *69*, 1097–1106.
16. Faust, C., Schumacher, A., Holdener, B., and Magnuson, T. (1995). The eed mutation disrupts anterior mesoderm production in mice. Development *121*, 273–285.
17. Bastian, H., and Gruss, P. (1990). A murine even-skipped homologue, Evx *1*, is expressed during early embryogenesis and neurogenesis in a biphasic manner. EMBO J. *9*, 1839–1852.
18. Crossley, P.H., and Martin, G.R. (1995). The mouse Fgf8 gene encodes a family of polypeptides and is expressed in regions that direct outgrowth and patterning in the developing embryo. Development *121*, 439–451.
19. Varlet, I., Collignon, J., and Robertson, E.J. (1997). nodal expression in the primitive endoderm is required for specification of the anterior axis during mouse gastrulation. Development *124*, 1033–1044.
20. Collignon, J., Varlet, I., and Robertson, E.J. (1996). Relationship between asymmetric nodal expression and the direction of embryonic turning. Nature *381*, 155–158.
21. Belo, J.A., Bouwmeester, T., Leyns, L., Kertesz, N., Gallo, M., Follettie, M., and De Robertis, E.M. (1997). Cerberus-like is a secreted factor with neutralizing activity expressed in the anterior primitive endoderm of the mouse gastrula. Mech. Dev. *68*, 45–57.
22. Dubois, A., Grieve, K., Moneron, G., Lecaque, R., Vabre, L., and Boccara, A.C. (2003). Ultrahigh-resolution full-field optical coherence tomography. Appl. Opt., in press.
23. Vabre, L., Dubois, A., and Boccara, A.C. (2002). Thermal-light full-field optical coherence tomography. Opt. Lett. *27*, 530–533.
24. Downs, K.M., and Davies, T. (1993). Staging of gastrulating mouse embryos by morphological landmarks in the dissecting microscope. Development *118*, 1255–1266.
25. Lawson, K.A., Meneses, J.J., and Pedersen, R.A. (1991). Clonal analysis of epiblast fate during germ layer formation in the mouse embryo. Development *113*, 891–911.
26. Rosner, M.H., Vigano, M.A., Ozato, K., Timmons, P.M., Poirier, F., Rigby, P.W., and Staudt, L.M. (1990). A POU-domain transcription factor in early stem cells and germ cells of the mammalian embryo. Nature *345*, 686–692.
27. Rodriguez, T.A., Casey, E.S., Harland, R.M., Smith, J.C., and Beddington, R.S. (2001). Distinct enhancer elements control Hex expression during gastrulation and early organogenesis. Dev. Biol. *234*, 304–316.
28. Tam, P.P. (1998). Postimplantation mouse development: whole embryo culture and micro- manipulation. Int. J. Dev. Biol. *42*, 895–902.
29. Oulad-Abdelghani, M., Chazaud, C., Bouillet, P., Mattei, M.G., Dolle, P., and Chambon, P. (1998). Stra3/lefty, a retinoic acid-inducible novel member of the transforming growth factor-beta superfamily. Int. J. Dev. Biol. *42*, 23–32.
30. Norris, D.P., Brennan, J., Bikoff, E.K., and Robertson, E.J. (2002). The Foxh1-dependent autoregulatory enhancer controls the level of Nodal signals in the mouse embryo. Development *129*, 3455–3468.
31. Beck, S., Le Good, J.A., Guzman, M., Ben Haim, N., Roy, K., Beermann, F., and Constam, D.B. (2002). Extraembryonic proteases regulate Nodal signalling during gastrulation. Nat. Cell Biol. *4*, 981–985.
32. Smith, J. (1999). T-box genes: what they do and how they do it. Trends Genet. *15*, 154–158.
33. Russ, A.P., Wattler, S., Colledge, W.H., Aparicio, S.A., Carlton, M.B., Pearce, J.J., Barton, S.C., Surani, M.A., Ryan, K., Nehls, M.C., et al. (2000). Eomesodermin is required for mouse trophoblast development and mesoderm formation. Nature *404*, 95–99.
34. Gardner, R.L. (1999). Polarity in early mammalian development. Curr. Opin. Genet. Dev. *9*, 417–421.
35. Weber, R.J., Pedersen, R.A., Wianny, F., Evans, M.J., and Zernicka-Goetz, M. (1999). Polarity of the mouse embryo is anticipated before implantation. Development *126*, 5591–5598.
36. Bellairs, R. (1986). The primitive streak. Anat. Embryol. (Berl.) *174*, 1–14.
37. Leptin, M., Casal, J., Grunewald, B., and Reuter, R. (1992). Mechanisms of early Drosophila mesoderm formation. Dev. Suppl., 23–31.
38. Tremblay, K.D., Dunn, N.R., and Robertson, E.J. (2001). Mouse embryos lacking Smad1 signals display defects in extra-embryonic tissues and germ cell formation. Development *128*, 3609–3621.
39. Huang, D., Swanson, E.A., Lin, C.P., Schuman, J.S., Stinson, W.G., Chang, W., Hee, M.R., Flotte, T., Gregory, K., Puliafito, C.A., et al. (1991). Optical coherence tomography. Science *254*, 1178–1181.
40. Mesnard, D., Filipe, M., Belo, J.A., and Zernicka-Goetz, M. (2004). The anterior-posterior axis emerges respecting the morphology of the mouse embryo that changes and aligns with the uterus before gastrulation. Curr. Biol. *14*, this issue, 184–196.